THE JOURNAL OF PHYSICAL CHEMISTRY B LETTERS

2008, *112,* 9557–9560
Published on Web 07/18/2008

Confinement-Dependent Below-Gap State in PbS Quantum Dot Films Probed by Continuous-Wave Photoinduced Absorption

Jian Zhang and Xiaomei Jiang*

Department of Physics, University of South Florida, Tampa, Florida 33620

Received: May 28, 2008; Revised Manuscript Received: July 7, 2008

We have measured continuous-wave (cw) photoinduced absorption (PA) spectra of PbS quantum dot (QD) films with four different sizes over a spectral range of 0.25−0.5 eV at $T = 10$ K. The PA spectrum shows a strong asymmetric IR absorption peak (IR-PA). Both the peak position and shape of this IR-PA indicate distinct confinement dependence. Combining with results of interband transitions and Stokes shift, we assign this IR-PA to a transition from a well-defined below-gap state to the second excitonic level (1P). By measuring the frequency dependence of this IR-PA, we estimate the lifetime of this below-gap state to be around several microseconds. Possible interpretations of the origin of this below-gap state are given. This transition could potentially be used to monitor photogenerated charge transfer in such QD systems.

I. Introduction

In recent years, extensive research activities have been going on with IV−VI semiconductor nanocrystals such as PbSe or PbS quantum dots (QDs). Their relatively large quantum confinement resulting from their big exciton Bohr radii makes these QDs excellent candidates for fundamental studies.[1–3] Because of their unique optical properties (i.e., size-tunable absorptions, large optical and dielectric constants, and high luminescence in IR range), these QDs find numerous applications in the area of telecommunications,[4] imaging in the biological transparent region,[5] effective infrared photodetectors,[6] and photovoltaic devices.[7–9] Because of the usually incomplete surface passivation of nanocrystals,[10] the presence of trap states below the optical gap in QDs largely modifies their optical and electronic properties; therefore the need to further investigate these trap states is worthwhile.

Continuous-wave (cw) photoinduced absorption (PA) spectroscopy has been a successful tool to study long-lived, subgap photoexcitations.[11] Our earlier work on cw PA of a 4 nm PbS QD film on glass substrate shows the presence of a photogenerated local electric field caused by trapped charges of QDs.[12] Motivated by the observation there, we extend our PA study to a spectral range below the QD bandgap by measuring PbS QD films on sapphire substrate. We expect to see photoinduced subgap transition from the trap state upon photoexcitation.

In this report, we demonstrate the cw PA spectra of a confinement-dependent below-gap state (BGS) in the spectral range from 0.25 to 0.5 eV, in PbS QD films with four different sizes (diameter from 2 to 5 nm). A typical PA contains a broad asymmetric photoinduced IR absorption (IR-PA), whose peak position and shape bear size-dependent characteristics. We interpret this IR-PA as being due to a transition from a BGS to the $1P_e$ excitonic level. Frequency dependence of such IR-PA has been measured, and the lifetime of this BGS is estimated to be around 2 μs.

* Corresponding author. E-mail: xjiang@cas.usf.edu.

II. Experimental Methods

All PbS QDs used in this study were purchased from Evident Technologies, Inc. These colloidal QDs were capped by oleic acid and stored in toluene solution. Four sizes of dots were chosen: 2.2, 2.5, 4.2, and 5.3 nm. The original QD solution with a concentration of 10 mg/mL was dried by blowing N_2 gas; after that, the same amount of chloroform was added to keep the concentration unchanged. QD film was made by immediately drop-casting the chloroform solution onto the sapphire substrate, which was cleaned in acetone and then 2-propanol in an ultrasonic bath, and then wet by chloroform. The average film thickness was around 500 nm (measured by a Tencor Alphastep 200 Profilometer). The as-cast film was left in a glovebox overnight, then kept in dynamic vacuum for 2 h before measurements. All the data were taken at 10 K (achieved in a Janis closed-cycle refrigerator cryostat) unless otherwise specified. All measured spectra were repeatable on films with a smooth morphology.

We apply the cw PA technique to investigate the long-lived photoexcitations in the PbS QD films. The pump beam is provided by the 488 nm line (2.54 eV) from a cw Ar^+ laser, with an optical chopper for photomodulation. A tungsten−halogen lamp is used to probe the modulated changes, ΔT, in transmission, T. The PA signal is expressed by $-\Delta T/T = \Delta\alpha d$, where α is absorption coefficient, and d is the film thickness.

A lock-in amplifier is employed to amplify the signal from photodetectors (silicon or InSb), with the reference frequency taken from the chopper controller. A Newport Oriel Cornerstone 1/4 m monochromator is used together with various diffraction gratings and optical filters to span the spectrum from 0.2 to 3.0 eV. Absorption and photoluminescence (PL) measurements are carried out on the same setup. In this report, a total pump power of 250 mW (i.e., power density of 150 mW/cm^2 on sample) and a modulation frequency of 400 Hz are used unless otherwise specified.

10.1021/jp8047295 CCC: $40.75

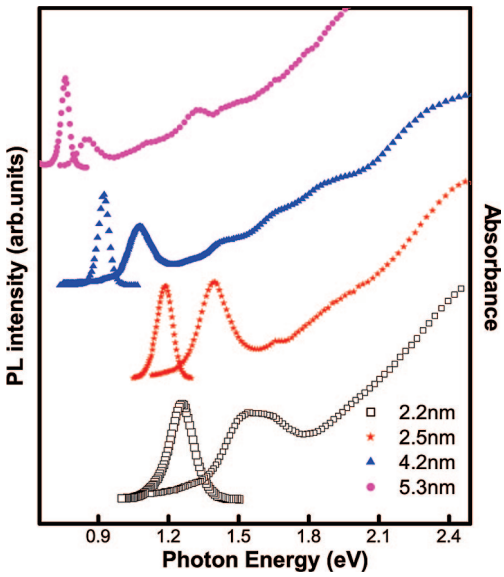

Figure 1. PL (left) and absorption (right) spectra for four different sizes (2.2−5.3 nm in diameter) of PbS QD films on sapphire measured at $T = 10$ K. Excitation is at a photon energy of 2.54 eV from a cw Ar^+ laser with intensity of 150 mW/cm^2. The baseline of the spectrum for each size was shifted vertically for clarity.

TABLE 1: Summary of Confinement-Dependent Transition Energies in PbS QD Films[a]

QD size	E_1	E_2	PL	Δ_s[b]	δ_1[c]	IR-PA	T_1[d]
2.2	1542	2026	1258	284	242	464	526
2.5	1395	1897	1199	196	251	426	448
4.2	1075	1423	925	150	174	332	324
5.3	853	1119	761	92	133	261	225

[a] Δ_s is the Stokes shift, δ_1 is the energy difference between $1P_e$ and $1S_e$, and T_1 is the transition from the BGS to the $1P_e$ level. All three quantities are calculated based on measured values. The size of the QD is denoted by its diameter in units of nm, and the unit for all energies is meV. [b] Calculated as $E_1 - E_{PL}$. [c] Calculated as $(E_2 - E_1)/2$. [d] Calculated as $\Delta_s + \delta_1$.

III. Results

Figure 1 represents the low-temperature ($T = 10$ K) PL and absorption spectra of four different sizes (2.2−5.3 nm) of PbS QD films on sapphire. Both absorption and PL show size-dependent features reflecting the quantum confinement effects. Up to four well-resolved interband transitions can be seen in the absorption spectra for larger size dots, which is consistent with a narrow distribution of sizes (<5%) for the PbS QDs studied here.

The PL peak has a Gaussian shape with a full width at half-maximum (fwhm) comparable to the first excitonic absorption peak, indicating that the emission comes from a well-defined single quantum state. Relatively large Stokes shifts (denoted by Δ_s) are present for all four films, and Δ_s decreases with increasing size (i.e., weaker quantum confinement). Δ_s is 92 meV for the 5.3 nm dot and 284 meV for the 2.2 nm dot (Table 1). Measurements of PL in diluted solution (0.7 mg/mL) for all four sizes of QDs demonstrate similarly large Stokes shifts, which eliminates the possibility of a dominant role from Förster energy transfer as formerly reported.[13] We hereby attribute the large Stokes shift as being due to a BGS. Large Stokes shift were previously reported in PbS QD films[14,15] and explained by the presence of a trap state.[16] Nevertheless, other possibilities, such as band-edge energy level splitting recently reported in PbSe QDs,[17] can not be completely ruled out, although the calculated Stokes shift therein was several times smaller than we observed here.

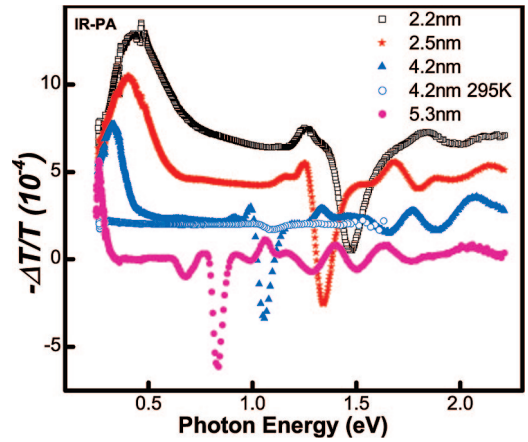

Figure 2. In-phase component, PA_{in}, of PA spectra for four different sizes of PbS QD films measured at $T = 10$ K. The zero line of each PA spectrum was shifted vertically for clarity. The lowest PB valley indicates the band edge of each QD. Also shown is the PA_{in} (open circle) of a 4.2 nm QD film at $T = 295$ K.

Figure 2 shows the in-phase component of PA (PA_{in}) for each QD film measured at $T = 10$ K. Each PA spectrum consists of two different features above and below the bandgap, E_g. At photon energies higher than E_g, a series of positive (PA) and negative (photoinduced bleaching (PB)) peaks are observed. This feature was interpreted as a linear Stark effect caused by a local electric field originated from the trapped charges of QDs.[12,18]

The broader IR-PA band lies in the near-infrared region from 0.25 to 0.5 eV, depending on QD size (Table 1). This IR-PA has an asymmetric shape with a high-energy side tail, and both its peak position and shape depend on the QD size. With increasing confinement, the peak is blue-shifted, and its bandwidth also increases. The temperature dependence of PA_{in} was measured in a range from 10 to 295 K (complete data not shown in this paper). This IR-PA and the above E_g PAs show similarly strong temperature dependence, and both features vanish at room temperature (see Figure 2 for a 4.2 nm QD film at 295 K (open circle)). Although the exact thermal activation energy of this IR-PA state has not yet been obtained, such a strong temperature dependence indicates that the transition most possibly comes from a shallow state. This derivation is further supported by its relatively short lifetime of several microseconds, as discussed below.

Figure 3 shows the in-phase (PA_{in}) and quadrature (PA_Q) components of the IR-PA peak varied with modulation frequency. It is clearly seen that the magnitude of PA_Q increases as the modulation frequency increases. However, even at $f =$ 20 KHz, which is the limit of our mechanical chopper, PA_Q is still much smaller than PA_{in}, indicating that the measurements have been conducted in the steady-state region. Assuming a single lifetime τ for the photoexcitation, we would expect a linear ratio of $PA_Q/PA_{in} = 2\pi\tau f$.[19] A good estimate of lifetime for the photoexcitaion could be extracted by a linear fitting of the ratio (PA_Q/PA_{in}). From the inset of Figure 3, we obtain $\tau \approx 2\ \mu$s. The PL decay times were previously measured in a solution of PbS QDs to be about 1−2 μs,[14,15] in good agreement with our estimated IR-PA state lifetime. This observation further validates that this BGS and the IR-PA state are essentially the same one, thus it lends strong support to the energy level diagram shown in the inset of Figure 4.

In Figure 4, we plot several relevant transition energies with respect to the first excitonic energy ($1S_h$ to $1S_e$, E_1). There are

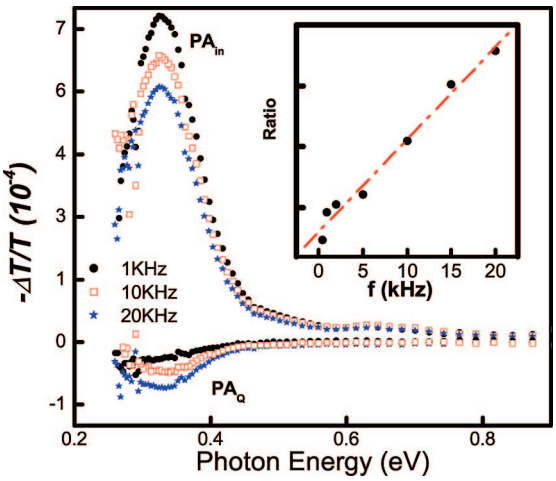

Figure 3. Frequency dependence of both the in-phase component (PA_{in}, upper) and the quadrature component (PA_Q, lower) of the PA spectrum for a 4.2 nm PbS QD film measured at $T = 10$ K. The inset shows the ratio of PA_Q and PA_{in} as a function of modulation frequency (400 to 20 KHz).

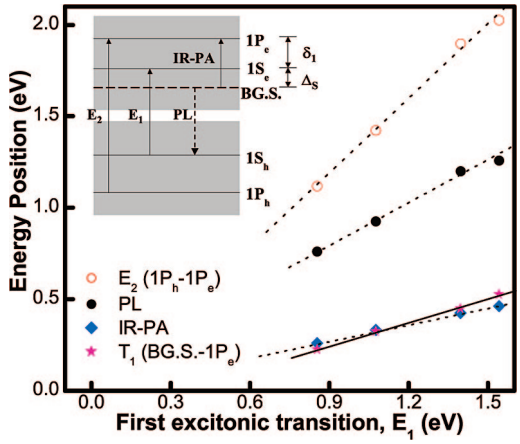

Figure 4. Plot of several relevant transition energies as a function of the first excitonic energy E_1. Both E_1 and PL are taken from Figure 1, whereas the second excitonic transition E_2 was taken from the second derivative of the absorbance spectra (not presented here). The IR-PA is the peak position of the IR-PA in Figure 2. Transition energy between the BGS and $1P_e$ is calculated by $\Delta_s + \delta_1$.

four sets of data: the second excitonic transition ($1P_h$ to $1P_e$, E_2), the PL, the IR-PA, and the transition from the BGS to the second excitonic energy level (BGS to $1P_e$, T_1). The inset of Figure 4 shows a schematic drawing of the involved energy levels. Although we only discuss the BGS associated with the electron, the same scenario should be applicable to the hole as well, since the effective masses of the electron and the hole in PbS are quite similar.

IV. Discussion

In addition to the above measured transition energies, we also list in Table 1 three calculated quantities, namely, the Stokes shift (Δ_s, difference between E_1 and PL), the energy difference (δ_1) between $1P_e$ and $1S_e$, and the transition T_1 (from BGS to $1P_e$). These three quantities are calculated by

$$\Delta_s = E_1 - E_{PL} \quad (1)$$

$$\delta_1 = (E_2 - E_1)/2 \quad (2)$$

$$T_1 = \Delta_s + \delta_1 \quad (3)$$

respectively.

It can be seen from Figure 4 that E_2, PL, and IR-PA all show linear relation with E_1, and they increase linearly with decreased size. A linear fitting of E_{PL} versus E_1 yields a slope of 0.75, indicating that the BGS is actually confinement related, i.e, the position of the BGS varies with respect to the bulk band edge.[16]

Now we begin the discussion about the possible origin of the observed IR-PA. Upon photoexcitation, followed by fast relaxation from higher excited levels (sub-picosecond),[20] there are several competing channels that could depopulate the $1S_e$ occupancy. One is the intraband transition, and the other is the fast relaxation of the $1S_e$ state to a lower-energy, longer lifetime BGS. Intraband transition from $1S_e$ to $1P_e$ could be a possible assignment for IR-PA. However, there is a problem with energy matching in that scenario: IR-PA appears at much higher energy than δ_1 for each size of QD film (Table 1). The close-match of transition energies has been a criterion for intraband transition assignment,[2,21] and it does not appear to be the case here. Instead, the excellent agreement between T_1 and the measured IR-PA shown in Figure 4 and Table 1 indicates the observed IR-PA could be a transition from a BGS to the second excitonic level $1P_e$.

The above analysis clearly states the presence of a well-defined BGS in the PbS QD films studied here. Its energy level is confinement-related, with an estimated lifetime of 2 μs. This BGS is responsible for the IR-PA in the mid-infrared range, as well as a largely red-shifted PL. Two different scenarios could each partially explain our observations. Scenario 1 is that this BGS belongs to a certain trap state, and this could explain the large Stokes shift. This scenario is supported by PL and PL excitation spectroscopy,[16] by electroabsorption spectroscopy,[22] and our previous demonstration of a photogenerated local electric field by trapped charges.[12] However, the characteristics of a conventional trap state do not completely go with the confinement-dependent, narrow emission band and relatively short lifetime observed here. It is possibly a peculiar trap state largely modified by the QD size, in that its lifetime is shorter than that of a conventional surface state or trap state (milliseconds), and the corresponding emission spectra are rather narrow.

Another possible interpretation is that it is a state related to band edge energy level splitting, as recently calculated in PbSe QDs.[17] This calculation based on intervalley coupling and exchange energy splitting predicted the existence of a dark exciton whose lifetime is size-dependent. A radiative lifetime as long as 875 ns at room temperature (possibly longer at low temperature) for 3 nm dots was calculated, comparable with our measured lifetime of the BGS. However, the Stokes shift calculated therein (about 80 meV) was several times smaller than what we observed here, and it also did not match the observed transition energy. Further work is needed for better scrutiny of its origin and nature.

V. Conclusions

In conclusion, we have measured the cw PA of four different sizes of PbS QD films on sapphire. We have observed distinct IR-PA at energies below the bandgap, and its lifetime is estimated to be 2 μs, in good agreement with the PL decay time measured elsewhere. We therefore link the emitting state to the IR-PA state, and the upper state is the $1P_e$ state, also because of the agreement between the relevant transition energies.

Both the peak position and shape of this IR-PA bear obvious quantum-confinement characteristics, which is hard to explain exclusively by a conventional trap state (i.e., surface state);

another interpretation of it being a dark exciton state is also possible. However, it might be a peculiar unconventional trap state modified by quantum confinement. This could explain the observed large Stokes shift, relatively short lifetime, and narrow emission spectra.

We speculate that this BGS could be used to monitor photoinduced charge transfer, similar to the case seen in conjugated polymer and fullerene systems.[23] Further investigation on the BGS could bring a positive outcome regarding the improvement of performance for optoelectronic devices based on these infrared nanocrystals.

Acknowledgment. We would like to thank Jason Lewis in our group for his help with the thickness measurement. We appreciatively acknowledge the financial support of this work by the ACS Petroleum Research Fund (PRF 47107-G10) and USF Grant No. NRG-R061717. J.Z. is grateful for support from USF Grant No. GFMMD03. We also appreciate Evident Technologies for selling the PbS QDs under the MTA agreement between Evident and USF.

References and Notes

(1) Kang, I.; Wise, F. W. *J. Opt. Soc. Am. B* **1997**, *14*, 1632–1646.
(2) Wehrenberg, B. L.; Wang, C.; Guyot-Sionnest, P. *J. Phys. Chem. B* **2002**, *106*, 10634–10640.
(3) An, J. M.; Franceschetti, A.; Dudiy, S. V.; Zunger, A. *Nano Lett.* **2006**, *6*, 2728–2735.
(4) Steckel, J. S.; Coe-Sullivan, S.; Bulovic, V.; Bawendi, M. G. *Adv. Mater.* **2003**, *15*, 1862–1866.
(5) Kim, S.; Lim, Y. T.; Soltesz, E. G.; De Grand, A. M.; Lee, J.; Nakayama, A.; Parker, J. A.; Mihaljevic, T.; Laurence, R. G.; Dor, D. M.; Cohn, L. H.; Bawendi, M. G.; Frangioni, J. V. *Nat. Biotechnol.* **2004**, *22*, 93–97.
(6) Konstantatos, G.; Howard, I.; Fischer, A.; Hoogland, S.; Clifford, J.; Klem, E.; Levina, L.; Sargent, E. H. *Nature* **2006**, *442*, 180–183.
(7) McDonald, S. A.; Konstantatos, G.; Zhang, S.; Cyr, P. W.; Klem, E. J. D.; Levina, L.; Sargent, E. H. *Nat. Mater.* **2005**, *4*, 138–142.
(8) Watt, A. A. R.; Blake, D.; Warner, J. H.; Thomsen, E. A.; Tavenner, E. L.; Rubinsztein-Dunlop, H.; Meredith, P. *J. Phys. D* **2005**, *38*, 2006–2012.
(9) Jiang, X.; Schaller, R. D.; Lee, S. B.; Pietryga, J. M.; Zakhidov, A. A.; Klimov, V. I. *J. Mater. Res.* **2007**, *22*, 2204–2210.
(10) Lobo, A.; Möller, T.; Nagel, M.; Borchert, H.; Hickey, S. G.; Weller, H. *J. Phys. Chem. B* **2005**, *109*, 17422–17428.
(11) Jiang, X. M.; Österbacka, R.; Korovyanko, O. J.; An, C. P.; Horovitz, B.; Janssen, R. A. J.; Vardeny, Z. V. *Adv. Funct. Mater.* **2002**, *12*, 587–597.
(12) Zhang, J.; Jiang, X. *Appl. Phys. Lett.* **2008**, *92*, 141108.
(13) Murray, C. B.; Kagan, C. R.; Bawendi, M. G. *Annu. Rev. Mater. Sci.* **2000**, *30*, 545–610.
(14) Warner, J. H.; Thomsen, E.; Watt, A. R.; Heckenberg, N. R.; Rubinutein-Dunlop, H. *Nanotechnology* **2005**, *16*, 175–179.
(15) Clark, S. W.; Harbold, J. M.; Wise, F. W. *J. Phys. Chem. C* **2007**, *111*, 7302–7305.
(16) Fernée, M. J.; Thomsen, E.; Jensen, P.; Rubinsztein-Dunlop, H. *Nanotechnology* **2006**, *17*, 956–962.
(17) An, J. M.; Franceschetti, A.; Zunger, A. *Nano Lett.* **2007**, *7*, 2129–2135.
(18) Gadermaier, C.; Menna, E.; Meneghetti, M.; Kennedy, W. J.; Vardeny, Z. V.; Lanzani, G. *Nano Lett.* **2006**, *6*, 301–305.
(19) Wohlgenannt, M.; Graupner, W.; Leising, G.; Vardeny, Z. V. *Phys. Rev. B* **1999**, *60*, 5321–5330.
(20) Schaller, R. D.; Agranovich, V. M.; Klimov, V. I. *Nat. Phys.* **2005**, *1*, 189–194.
(21) Krapf, D.; Kan, S.-H.; Banin, U.; Millo, O.; Saár, A. *Phys. Rev. B* **2004**, *69*, 073301.
(22) Klem, E. J. D.; Levina, L.; Sargent, E. H. *Appl. Phys. Lett.* **2005**, *87*, 053101.
(23) Yu, G.; Gao, J.; Hummelen, J. C.; Wudl, F.; Heeger, A. J. *Science* **1995**, *270*, 1789–1791.

JP8047295